Echo-Enabled X-Ray Vortex Generation

E. Hemsing and A. Marinelli

Phys. Rev. Lett. **109**, 224801 — Published 27 November 2012

DOI: 10.1103/PhysRevLett.109.224801

Echo-enabled x-ray vortex generation

E. Hemsing[1] and A. Marinelli[2]
[1] *SLAC National Accelerator Laboratory, Menlo Park, California 94025, USA and*
[2] *Department of Physics and Astronomy, UCLA, Los Angeles, California 90095, USA*

A technique to generate high-brightness electromagnetic vortices with tunable topological charge at EUV and x-ray wavelengths is described. Based on a modified version of echo-enabled harmonic generation (EEHG) for free-electron lasers, the technique uses two lasers and two chicanes to produce high-harmonic microbunching of a relativistic electron beam with a corkscrew distribution that matches the instantaneous helical phase structure of the x-ray vortex. The strongly correlated electron distribution emerges from an efficient three-dimensional recoherence effect in the EEHG transport line, and can emit fully coherent vortices in a downstream radiator for access to new research in x-ray science.

PACS numbers: 41.60.Cr, 42.60.Jf, 42.50.Tx, 42.65.Ky

Modern x-ray free-electron lasers (FELs) have become a remarkable tool for probing matter at Ångstrom length and femtosecond time scales with unprecedented brightness[1]. Generated by a relativistic beam of electrons, the FEL light frequency and distribution are tunable according to the electron beam (e-beam) energy, and coherent e-beam distribution, respectively. In most modern X-ray FELs, the amplification process starts from random noise in the e-beam distribution, which produces an almost fully transversely coherent fundamental mode, but one with limited temporal coherence. To achieve fully temporally and spatially coherent radiation, the echo-enabled harmonic generation (EEHG) scheme has been proposed [2, 3], and the concept experimentally demonstrated [4, 5], as a promising candidate to reach short wavelengths via efficient high-harmonic up-conversion. The standard EEHG scheme uses two modulators and two chicanes to generate longitudinal microbunching in the e-beam at the frequency $k = nk_1 + mk_2$, where k_1 and k_2 are the frequencies of the longer wavelength lasers in the modulating sections. High harmonics can be obtained by precise tuning of the modulation amplitudes and chicane dispersions. The transverse phase and intensity profile of the modulating lasers are assumed constant over the e-beam profile so that the final harmonic microbunching structure has no transverse spatial dependence. Because the light emitted by the e-beam will have a phase structure determined by the microbunching distribution, this facilitates emission into the Gaussian-like fundamental FEL mode, which is peaked on-axis and has an axisymmetric transverse phase profile.

There are, however, numerous theoretical and experimental contexts in which higher-order light beams provide access to a different class of phenomena. Of particular recent interest are optical vortices (OVs), or light beams that carry well-defined, discrete azimuthal phase about the axis of propagation. In such beams, the complex field goes like $e^{il\phi}$ where ϕ is the azimuthal coordinate, and l is an integer referred to as the topological charge. OVs have become a topic of intense scientific interest due to their intriguing properties [6–8]. Starting from the work of Allen [9], who showed that certain types of OV modes carry discrete values $l\hbar$ of orbital angular momentum (OAM) per photon, there has been considerable work exploring the interaction of OVs with matter [6]. OAM can be transferred to trapped particles and atoms [10–12]. OVs also have a corresponding ringlike intensity profile that can facilitate microscopy [13, 14], imaging [15], and optical pump schemes [16]. At x-rays, OAM modes have been proposed as a method to separate quadrupolar from dipolar electronic transitions at K-edges [17]. Beams with fractional topological charge (l non-integer) are also under investigation [18]. With these unique features, high-brightness x-ray OVs could open the door to new research for FELs in applications where the well-defined spatial intensity and phase variation can play a key role.

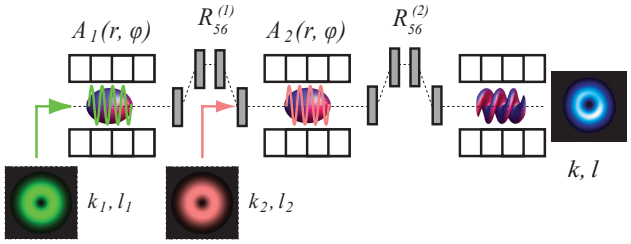

FIG. 1: General setup for echo-enabled optical vortex generation.

The generation of low order (small l) OAM light in x-ray FELs has been proposed previously in the context of harmonic emission[19] and emission at the fundamental frequency [20]. In the latter high-gain high mode generation (HGHMG) scheme, fully coherent OAM light is radiated from an e-beam with a corresponding helical microbunching distribution at the resonant FEL wavelength. This requires a coherent x-ray seed to perform the necessary modulation on the e-beam. To avoid this limitation, the technique explored in this Letter exploits

both the supreme harmonic upconversion efficiency of EEHG and the unique e-beam structure generated in HGHMG to produce helical microbunching at x-rays using conventional, longer wavelength lasers. The layout is shown in Fig. 1, and resembles that for EEHG. Here however, the energy modulation imposed on the e-beam in at least one of the modulators has a well-defined helical spatial dependence such that an electron's energy depends on it's spatial position in the beam. This occurs if the complex laser mode field profile is itself an OAM mode (as depicted), or, more generally, if the resonant phase bucket has a corkscrew geometry as in harmonics of helical undulators [21, 22]. After passage through the EEHG beam line, a helical density modulation appears through recoherence of the imprinted energy modulations as a function of the electron's spatial position. As a result, both the frequency and helical mode number l are converted through a process we call Echo-v. The final highly-correlated microbunched distribution can be tailored to emit specific OVs and frequency harmonics in the radiator through optimization of the modulation profile, amplitude, and dispersion.

A striking feature of the spatial recoherence effect in Echo-v is that it allows large up-conversion of the frequency and l mode either simultaneously, or independently. By upconverting both together, one can emit optical vortices with large l at high-harmonics. Alternately, large frequency harmonics can be generated without changing $|l|$, so that the helical distribution generated at one frequency to be passed to a vastly different frequency.

To calculate the bunching factor at the mode l, let the e-beam distribution at the entrance to the first modulator be given by $f_i(\mathbf{x}_\perp, p)$, where $\mathbf{x}_\perp = (r, \phi)$ are the radial and azimuthal coordinates, $p = (E - E_0)/\sigma_E$ is the scaled electron energy with respect to the central beam energy $E_0 = \gamma mc^2$, and σ_E is the rms energy spread. Consider the complex modulation amplitude in the first modulator to be of the form $A_1(\mathbf{x}_\perp) = \overline{A}_1(r)\exp(il_1\phi)$, where l_1 is an integer that describes the azimuthal phase variation across the profile, and $\overline{A}_1$ is the radially dependent field amplitude. At the exit of the first modulator section, the beam energy is modulated such that an electron acquires a new energy $p' = p + \overline{A}_1 \sin(k_1 z + l_1\phi)$ where $k_1 = 2\pi/\lambda_1$ is the laser frequency and z is the initial longitudinal position of the electron in the beam. (See Fig. 2) Note that the energy kick depends on the electron's transverse position (r, ϕ), and that the mathematical form of the modulating field is general in that it describes a modulation generated either by an OAM laser seed, or by harmonics [20, 22]. The beam then passes through a longitudinally dispersive section characterized by the matrix element $R_{56}^{(1)}$, which shifts the electron to the position z' according to $z' = z + B_1 p'/k_1$, where $B_1 = R_{56}^{(1)} k_1 \sigma_E / E_0$. The beam is then modulated by the second laser, with frequency $k_2 = 2\pi/\lambda_2$, in the second modulator according to the field distribution $A_2(\mathbf{x}_\perp) = \overline{A}_2(r)\exp(il_2\phi)$. The new energy is $p'' = p' + \overline{A}_2 \sin(k_2 z' + l_2\phi)$. The second chicane, with dispersion $R_{56}^{(2)}$, transforms the longitudinal position as, $z'' = z' + B_2 p''/k_1$, where $B_2 = R_{56}^{(2)} k_1 \sigma_E / E_0$. In terms of the final variables at the end of the last dispersive element, the e-beam bunching factor at the frequency k and at the azimuthal mode l is given by

$$b^{(l)}(k) = \left| \langle e^{-ikz'' - il\phi} f_f(\mathbf{x}_\perp, z'', p'') \rangle \right|, \tag{1}$$

where $f_f(\mathbf{x}_\perp, z'', p'')$ is the final e-beam distribution, and brackets denote averaging over the final coordinates. Transforming back to the initial coordinates, the exponential term is then,

$$\exp\left[-ikz'' - il\phi\right] = \sum_{n,m} e^{-ikz - il\phi - i\frac{k}{k_1} p(B_1 + B_2) + in(k_1 z + l_1\phi) + im(k_2 z + l_2\phi + K B_1 p)} \times J_n\left[mK\overline{A}_1 B_1 - \frac{k}{k_1}\overline{A}_1 (B_1 + B_2) \right] J_m\left(-\frac{k\overline{A}_2 B_2}{k_1} \right) \tag{2}$$

where $K = k_2/k_1$. Averaging over z for a long beam ($\gg k^{-1}$) picks out the dominant microbunching frequencies,

$$k \equiv ak_1 = nk_1 + mk_2, \tag{3}$$

where $a = n + mK$. This is precisely the same frequency conversion relation as EEHG. Here, however, there is also an l-mode conversion relation, found by integration over ϕ. Assuming an axisymmetric, uncorrelated initial e-beam distribution $f_i(\mathbf{x}_\perp, p) = (2\pi)^{-1/2} e^{-p^2/2} f_0(r)$, the

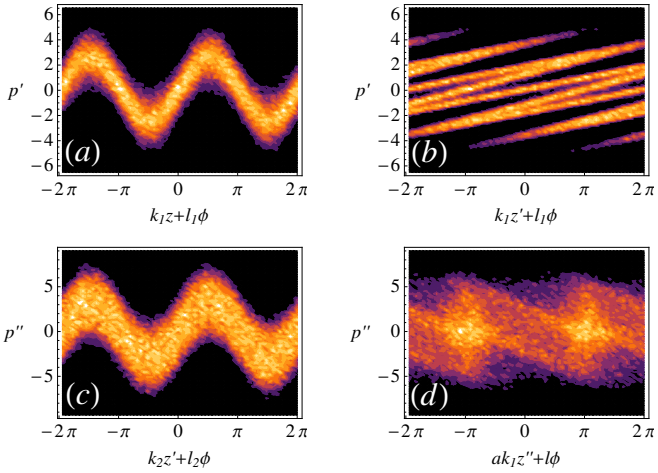

FIG. 2: Example evolution of correlated e-beam phase space after passage through (a) $l_1 = 1$ energy modulation, (b) $R_{56}^{(1)}$ of chicane 1, (c) $l_2 = 0$ energy modulation in modulator 2 and finally, (d) $R_{56}^{(2)}$ of chicane 2. The frequency up-converted $l = -1$ density modulation emerges through recoherence in the Echo-v process.

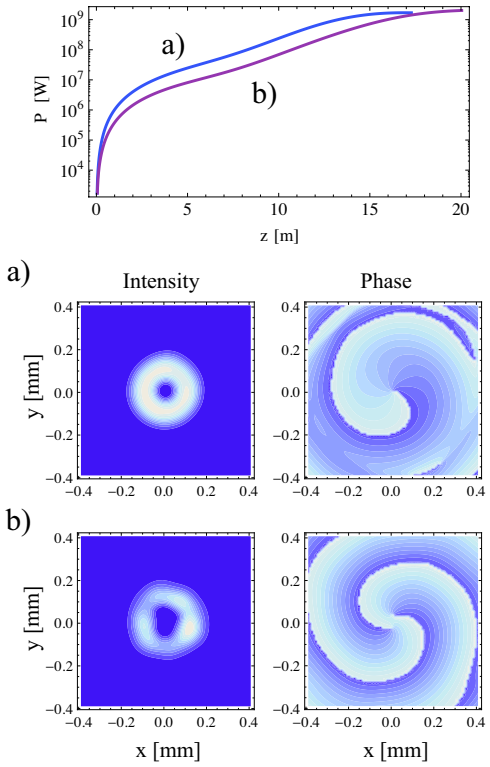

FIG. 3: High-gain FEL emission of OVs with a) $l = -1$ and b) $l = -2$, frequency up-converted from $\lambda_1 = \lambda_2 = 240$ nm lasers with $A_1 = A_2 = 5$. Dispersions of a) $B_1 = 8, B_2 = 0.22$ yield 8% at 6.15 nm for $(n, m) = (-1, 40)$ and b) $B_1 = 3.84, B_2 = 0.22$ yield 5% bunching at 6.32 nm for $(n, m) = (-2, 40)$. A 2 GeV, 1kA beam is assumed.

ϕ integral in (1) is straightforward, and the final azimuthal density mode excited in the beam has the same up-conversion as the frequency:

$$l = nl_1 + ml_2. \tag{4}$$

One can therefore convert both the frequency and azimuthal mode number of the microbunched distribution in Echo-v. The final bunching factor is expressed in general as,

$$b^{(l)}_{n,m} = \left| e^{-\xi^2/2} \int J_n\left(\overline{A}_1\xi\right) J_m\left(-a\overline{A}_2B_2\right) f_0(r) r dr \right|, \tag{5}$$

where $\xi = -(nB_1 + aB_2)$. If the transverse variation of the fields is negligible over the e-beam such that $l_1, l_2 = 0$, $\overline{A}_1 = A_1$ and $\overline{A}_2 = A_2$, this reduces to the 1D expression in [2] for standard EEHG. With $\overline{A}_2 = B_2 = 0$, the general formula for HGHMG is recovered [20].

Among the numerous possible combinations of helical mode numbers l_1 and l_2 and harmonic numbers n and m, two examples illustrate the primary aspects. We first examine the frequency upconversion of a low-order helical microbunching distribution for the generation coherent low-order OAM modes at short wavelengths. Consider an $l_1 = 1$ modulation in the first stage of Fig 1 from a field of the form $\overline{A}_1(r) = A_1(\sqrt{2}r/w_0)^{|l_1|}e^{-r^2/w_0^2}$, where w_0 is the laser spot size. The e-beam is then modulated in the second stage by a laser with $l_2 = 0$. From Eq. (4) the final azimuthal mode number is given by $l = nl_1$, and thus does not depend on the potentially large harmonic number m of the frequency up-conversion. As with EEHG, for $m \gg 1$, the bunching factor is maximized when $n = -1$ and B_1 and B_2 have the same sign. Thus, the final mode number is $l = nl_1 = -1$. Assuming negligible transverse variation in the second stage ($\overline{A}_2 = A_2$) the bunching factor in (5) becomes

$$b^{(-1)}_{-1,m} = \left| e^{-\xi^2/2} J_m\left(-aA_2B_2\right) \int J_1\left(\overline{A}_1\xi\right) f_0(r) r dr \right|. \tag{6}$$

To find the maximum value of bunching and the scaling for harmonics $m > 4$, we note (as [3]) that the function J_m has a maximum value of $0.67/m^{1/3}$ when $aA_2B_2 \simeq m + 0.81m^{1/3}$. With a Gaussian e-beam distribution $f_0(r) = \sigma_x^{-2}e^{-r^2/2\sigma_x^2}$, the integral is maximized when the laser spot size matches the e-beam size, $w_0 = 2\sigma_x$. At this value, analysis shows that the peak of $|e^{-\xi^2/2}\int J_1\left(\overline{A}_1\xi\right) f_0(r) r dr|$ grows almost linearly from 0 to 0.4 for $A_1 < 4$ before leveling off asymptotically at 0.53 when A_1 grows to infinity. In this limit, the maximum bunching factor for the $l = -1$ helical mode at frequency $k = -k_1 + mk_2$ is

$$b^{(-1)}_{-1,m} \approx \frac{0.36}{m^{1/3}}, \tag{7}$$

which has the same scaling with m as standard EEHG. This high efficiency enables a $l_1 = 1$ helical mode structure, imparted to an e-beam at long wavelengths, to be strongly upshifted in frequency to generate an $l = -1$ mode at short wavelengths. Examples are shown in Fig. 3 from Genesis simulations [23], where an $l_1 = 1$ modulation at λ_1=240 nm is frequency upshifted to produce GW-level soft x-ray OVs at 6 nm.

Note that the final mode l has the opposite sign as l_1 by virtue of the sign of n. This ability to transform between different azimuthal mode numbers is a key feature of the 3D echo recoherence effect, and is highlighted by examining a second scenario which performs simultaneous large up-conversion of both the frequency and the l mode number. Consider a reversal of the previous arrangement, where the helical modulation is instead performed in the second modulator. The first modulation has no transverse dependence ($l_1 = 0$), so that the final azimuthal mode number is then $l = ml_2$, which can be made large in $m \gg 1$ harmonic upconversion. Taking

$l_2 = 1$, the final bunching factor is now given by

$$b^{(m)}_{-1,m} = \left| e^{-\xi^2/2} J_1\left(A_1\xi\right) \int J_m\left(-a\overline{A}_2 B_2\right) f_0(r) r dr \right|. \tag{8}$$

Maximizing with $w_0 = 2\sigma_x$ for the second laser, the integral term peaks at a value of $0.62/m^{1/2}$ when $aA_2B_2 \simeq 1.65m + 2m^{1/3}$. Combined with the maximum value 0.58 of the function $e^{-\xi^2/2}J_1\left(A_1\xi\right)$ for large A_1, the bunching factor in this scheme scales with the harmonic number as

$$b^{(m)}_{-1,m} \approx \frac{0.36}{m^{1/2}}. \tag{9}$$

In this arrangement, both the microbunching frequency and l mode azimuthal bunching factor are up-converted by m, and the beam can emit fully coherent, high-brightness vortices with high mode numbers $l = m \gg 1$. Fig. 4 shows an example of the bunching spectrum for a finite-length e-beam where multiple closely spaced frequencies are excited for the nearby m values. In this scheme, each frequency peak corresponds to a distinct l mode. Thus, a narrowband radiator tuned to pick out a single frequency peak will emit a coherent vortex with a corresponding value of topological charge. Because the peaks are closely spaced, this suggests a tunable frequency/mode configuration.

Whereas low-order l modes can be strongly amplified by the FEL process, large l modes are not amplified due to their greater emission angles and weaker coupling. They can be emitted superradiantly however, in an undulator, from a metal foil [24], or other suitable radiator. In this context, Echo-v may also be used in other devices such as synchrotrons, where the low-peak-current prevents gain in other transverse modes from spoiling the vortex purity. In the absence of high-gain, the coherent far-field angular emission power spectrum is calculated from $U_{k,\Omega} = U^e_{k,\Omega} N_0^2 |F|^2$, where N_0 is the number of electrons, $U^e_{k,\Omega}$ is the single electron emission kernel for a given radiator, $F(k,\theta,\varphi) = \int f_f(\mathbf{x}'', p'') \exp[-ik\mathbf{n}\cdot\mathbf{x}'']d\mathbf{x}''dp''$ is the e-beam form factor, and $d\Omega = \sin\theta d\theta d\varphi$ is the solid angle. At the frequency $k = -k_1 + mk_2$ and mode $l = m$, the form factor is,

$$F_{-1,m} = e^{-\xi^2/2 - im(\varphi - \pi/2)} J_1\left(A_1\xi\right) \int J_m\left(-a\overline{A}_2 B_2\right) J_m\left(ak_1 r\sin\theta\right) f_0(r) r dr. \tag{10}$$

Emission is maximized when the peaks of the functions in the integrand overlap. This occurs at a forward angle near $\theta \approx aA_2B_2\sqrt{2}/w_0 k\sqrt{e} \approx (1.65m + 2m^{1/3})/\sigma_x k\sqrt{2e}$ for $m > 4$, which can be adjusted with the beam size to lie within the single electron emission distribution of the radiator in order to avoid strong suppression.

Several physical considerations remain for optimization of this scheme in practice, including the effects of laser spectral phase [25] and mode purity, and alignment.

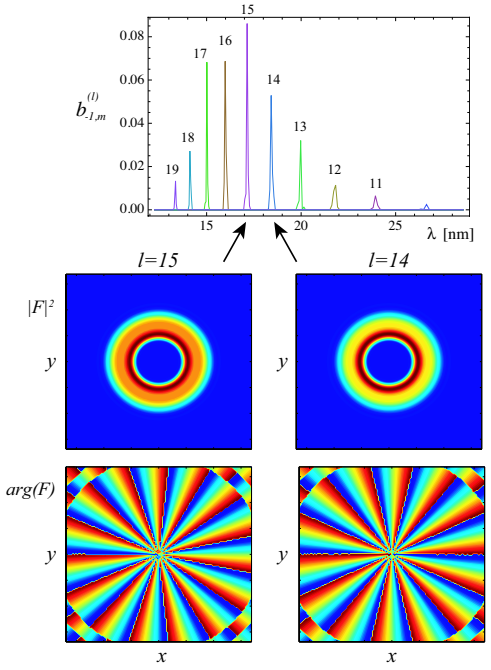

FIG. 4: Microbunching frequency and mode spectrum for $(n,m) = (-1,15)$ with $l_1 = 0$ and $l_2 = 1$ ($\lambda_1 = \lambda_2 = 240$ nm, $A_1 = A_2 = 5$, B1=5.6 and B2=0.42) The different frequency peaks around 17 nm in a finite length beam are also different l-modes near $l = 15$, indicated both by the intensity $|F|^2$ and phase $arg(F)$ of the e-beam form factor, integrated over the narrow peak.

Also, helically modulating the beam generates transverse variation in the longitudinal momentum, which gives rise to longitudinal variation in the transverse momentum by the deflection theorem [26]. At the exit of the first modulator, for example, the transverse electron momenta $\beta_x = dx/dz$ and $\beta_y = dy/dz$ are changed by $\Delta\beta_{x,(y)} = \frac{\sigma_E}{E_0}\int \partial_{x,(y)}\Delta p' dz$ where $\Delta p' = \overline{A}_1(r)\sin(k_1 z + l_1\phi)$. The result is a correlated emittance increase which can affect the e-beam transport dynamics if it is comparable to the intrinsic e-beam emittance. A straightforward calculation gives the induced angular spread as,

$$\langle(\Delta\beta_{x,(y)})^2\rangle = \left(\frac{\sigma_E A_1}{E_0 k_1 \sigma_x}\right)^2 \frac{l_1!}{8\alpha^{l_1+2}}\left[2l_1\alpha(\alpha-1) + l_1 + 1\right] \tag{11}$$

where $l_1 = |l_1|$ and $\alpha = 1 + w_0^2/4\sigma_x^2$. The last term is the contribution of the finite sized laser spot on the e-beam profile, which exists even in standard EEHG for l_1=0, but vanishes for large laser profiles ($\alpha \gg 2$). Overall, Eq. (11) can be neglected if $\langle(\Delta\beta_{x,(y)})^2\rangle / \langle\beta^2_{x,(y)}\rangle \ll 1$, which is easily satisfied in high-brightness e-beams. Finally, not only does the long term memory of the correlated phase space have to be preserved to obtain the high-harmonic values, but the highly correlated *helical* structure is also susceptible to wash out. Optimization requires precise tuning of the betatron phase advance to be a multiple of

π in order to reestablish the 3D structure at the radiator.

In summary, we have proposed a technique based on a combination of EEHG and HGHMG to efficiently generate intense, tunable x-ray vortices in modern electron accelerators using conventional lasers. Such exotic beams have potential to open new areas of research in x-ray science.

The authors thank C. Hast and D. Xiang for discussions. Work supported by U.S. DOE under Contract Nos. DE-AC02-76SF00515 and DE-FG02-07ER46272.

[1] P. Emma et al., Nat Photon **4**, 641 (2010).
[2] G. Stupakov, Phys. Rev. Lett. **102**, 074801 (2009).
[3] D. Xiang and G. Stupakov, Phys. Rev. ST Accel. Beams **12**, 030702 (2009).
[4] D. Xiang, E. Colby, M. Dunning, S. Gilevich, C. Hast, K. Jobe, D. McCormick, J. Nelson, T. O. Raubenheimer, K. Soong, et al., Phys. Rev. Lett. **105**, 114801 (2010).
[5] D. Xiang, E. Colby, M. Dunning, S. Gilevich, C. Hast, K. Jobe, D. McCormick, J. Nelson, T. O. Raubenheimer, K. Soong, et al., Phys. Rev. Lett. **108**, 024802 (2012).
[6] M. Padgett and R. Bowman, Nat Photon **5**, 343 (2011).
[7] G. Molina-Terriza, J. P. Torres, and L. Torner, Nat Phys **3**, 305 (2007).
[8] M. R. Dennis, R. P. King, B. Jack, K. O/'Holleran, and M. J. Padgett, Nat Phys **6**, 118 (2010).
[9] L. Allen, M. W. Beijersbergen, R. J. C. Spreeuw, and J. P. Woerdman, Phys. Rev. A **45**, 8185 (1992).
[10] M. E. J. Friese, J. Enger, H. Rubinsztein-Dunlop, and N. R. Heckenberg, Phys. Rev. A **54**, 1593 (1996).
[11] A. R. Carter, M. Babiker, M. Al-Amri, and D. L. Andrews, Phys. Rev. A **73**, 021401 (2006).
[12] M. F. Andersen, C. Ryu, P. Clade, V. Natarajan, A. Vaziri, K. Helmerson, and W. D. Phillips, Phys. Rev. Lett. **97**, 170406 (2006).
[13] A. Jesacher, S. Fürhapter, S. Bernet, and M. Ritsch-Marte, Phys. Rev. Lett. **94**, 233902 (2005).
[14] P. Török and P. Munro, Opt. Express **12**, 3605 (2004).
[15] B. Jack et al., Phys. Rev. Lett. **103**, 083602 (2009).
[16] J. W. R. Tabosa and D. V. Petrov, Phys. Rev. Lett. **83**, 4967 (1999).
[17] M. van Veenendaal and I. McNulty, Phys. Rev. Lett. **98**, 157401 (2007).
[18] S. S. R. Oemrawsingh, A. Aiello, E. R. Eliel, G. Nienhuis, and J. P. Woerdman, Phys. Rev. Lett. **92**, 217901 (2004).
[19] S. Sasaki and I. McNulty, Phys. Rev. Lett. **100**, 124801 (2008).
[20] E. Hemsing, A. Marinelli, and J. B. Rosenzweig, Phys. Rev. Lett. **106**, 164803 (2011).
[21] In this case, the helical geometry emerges naturally using a simple Gaussian laser profile, making helically polarized modulators attractive alternatives to performing the optical mode conversion on the laser directly.
[22] E. Hemsing, P. Musumeci, S. Reiche, R. Tikhoplav, A. Marinelli, J. B. Rosenzweig, and A. Gover, Physical Review Letters **102**, 174801 (2009).
[23] S. Reiche, Nuclear Instruments and Methods in Physics Research A **429**, 243 (1999).
[24] E. Hemsing and J. B. Rosenzweig, Journal of Applied Physics **105**, 093101 (2009).
[25] D. Ratner, A. Fry, G. Stupakov, and W. White, Phys. Rev. ST Accel. Beams **15**, 030702 (2012).
[26] W. K. H. Panofsky and W. A. Wenzel, Review of Scientific Instruments **27**, 967 (1956).